J. Nonlinear Sci. Vol. 17: pp. 59–83 (2007)
DOI: 10.1007/s00332-005-0723-4

Journal of
Nonlinear
Science

Quasiperiodic Dynamics in Bose-Einstein Condensates in Periodic Lattices and Superlattices

M. van Noort,[1] Mason A. Porter,[2] Y. Yi,[3] and S.-N. Chow[3]

[1] Department of Mathematics, Imperial College, London SW7 2AZ, UK
m.vannoort@imperial.ac.uk

[2] Department of Physics and Center for the Physics of Information, California Institute of Technology, Pasadena, CA 91125, USA
mason@caltech.edu

[3] Center for Dynamical Systems and Nonlinear Studies, School of Mathematics, Georgia Institute of Technology, Atlanta, GA 30332, USA
{yi,chow}@math.gatech.edu

Received July 23, 2005; revised manuscript accepted for publication May 31, 2006
Online publication November 9, 2006
Communicated by R. S. MacKay

Summary. We employ KAM theory to rigorously investigate quasiperiodic dynamics in cigar-shaped Bose-Einstein condensates (BEC) in periodic lattices and superlattices. Toward this end, we apply a coherent structure ansatz to the Gross-Pitaevskii equation to obtain a parametrically forced Duffing equation describing the spatial dynamics of the condensate. For shallow-well, intermediate-well, and deep-well potentials, we find KAM tori and Aubry-Mather sets to prove that one obtains mostly quasiperiodic dynamics for condensate wave functions of sufficiently large amplitude, where the minimal amplitude depends on the experimentally adjustable BEC parameters. We show that this threshold scales with the square root of the inverse of the two-body scattering length, whereas the rotation number of tori above this threshold is proportional to the amplitude. As a consequence, one obtains the same dynamical picture for lattices of all depths, as an increase in depth essentially affects only scaling in phase space. Our approach is applicable to periodic superlattices with an arbitrary number of rationally dependent wave numbers.

Key words. Hamiltonian dynamics, Bose-Einstein condensates, KAM theory, Aubry-Mather theory

MSC numbers. 37J40, 70H99, 37N20

PAC numbers. 05.45.-a, 03.75.Lm, 05.30.Jp, 05.45.Ac, 03.75.Nt

1. Introduction

Bose-Einstein condensates (BECs) have generated considerable excitement in the physics community both because their study allows one to explore new regimes of fundamental physics and because of their eventual engineering applications. They constitute a macroscopic quantum phenomenon, and their analysis has already led to an increased understanding of phenomena such as superfluidity and superconductivity. Of particular interest are BECs in optical lattices (periodic potentials), which have already been used to study Josephson effects [1], squeezed states [49], Landau-Zener tunneling and Bloch oscillations [43], and the transition between superfluidity and Mott insulation [13], [24], [61]. With each lattice site occupied by one alkali atom in its ground state, BECs in periodic potentials also show promise as registers for quantum computers [57], [63].

In the present paper, we generalize recent work on near-autonomous dynamics in BECs [52], [53] to study quasiperiodic behavior in BECs in periodic lattices, which can have shallow, intermediate, or deep wells. We present our methodology and results in Section 1.1. In Section 2, we discuss the physics of BECs and use a coherent structure ansatz to derive a parametrically forced Duffing oscillator describing the spatial dynamics of the condensate. The quasiperiodic dynamics of parametrically forced Duffing oscillators is rigorously investigated in Section 3. Sections 3.1 and 3.2 then describe applications to BECs in periodic lattices and periodic superlattices, respectively. The KAM theorem used in this analysis is proven in Section 4. Finally, we summarize and discuss our results in Section 5.

1.1. Methodology and Results

The spatial dynamics of standing waves in BECs in periodic optical lattices can be described by a parametrically forced Duffing equation, where the periodic forcing is given by an external potential due to the lattice [10], [52], [53]. This gives a $1\frac{1}{2}$-degree-of-freedom Hamiltonian system. We use KAM theory and Aubry-Mather theory to study its quasiperiodic dynamics. Previous KAM studies in BECs took a heuristic approach and considered only near-autonomous situations [52], [53]. The approach of this paper, however, is especially versatile in that shallow, deep, and intermediate lattice wells can all be considered using the same mathematical framework. That is, we consider the near-autonomous and far-from-autonomous settings simultaneously.

Theorem 6 proves that for any (analytic) external periodic potential, any negative two-body scattering length, and any chemical potential, one obtains mostly two-quasiperiodic dynamics for condensate wave functions of sufficiently large amplitude, where the minimal amplitude depends on the experimentally adjustable BEC parameters. In particular, the threshold amplitude is proportional to the reciprocal of the square root of the scattering length. Any two-quasiperiodic wave function above the threshold has one fixed frequency and one proportional to its amplitude. We also demonstrate numerically that one obtains the same dynamical picture for lattices of all depths, as an increase in lattice amplitude essentially affects only scaling in phase space. These numerical results support the theoretically predicted scaling of the threshold amplitude. Our theorem applies to periodic superlattices with an arbitrary number of rationally dependent wave numbers.

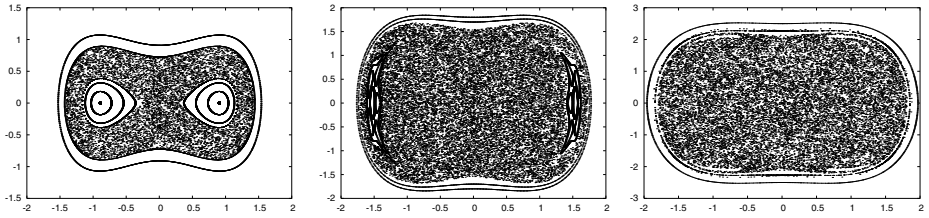

(a) (b) (c)

Fig. 1. Phase portraits of the Poincaré map P for the example of Section 3.1, with horizontal axis R and vertical axis S. In this case, the Hamiltonian is of the form $H = \frac{1}{2}S^2 - \frac{1}{2}[1+V_1\cos(\xi)]R^2 + \frac{1}{4}R^4$. Observe the invariant curves for large R in these figures. Generically, the invariant manifolds of the central saddle point intersect transversally, creating a homoclinic tangle and thereby implying the existence of horseshoes of measure zero. By conjecture, the closure of these horseshoes is a "chaotic sea" of positive measure, corresponding to the dots in the figures. As the size of the perturbation V_1 is increased to $+\infty$, the size of each of the remaining integrable islands vanishes, but their total measure remains $O(1)$. The values of V_1 are (a) $V_1 = 0.1$, (b) $V_1 = 0.5$, and (c) $V_1 = 1$.

The system we investigate is given by a Hamiltonian of the form $H(R, S, \xi) = \frac{1}{2}S^2 + U(R, \xi)$, where $|R|$ is the amplitude of the wave function, R and S are conjugate variables, $\xi \in \mathbb{R}/\mathbb{Z}$, and $\xi' = 1$. The function U is a polynomial in R and one-periodic in ξ. We also consider its Poincaré map, defined to be the return map on the section $\xi = 0$.

One can show that such systems have invariant tori sufficiently far from the origin $(R, S) = (0, 0)$ even when they are far from autonomous (that is, even when H is a large perturbation of an ξ-independent system). In the present case, this implies the existence of invariant tori for any optical lattice depth. The key condition is that $U(R, \xi)/R^2 \to +\infty$ as $R \to \pm\infty$, as this guarantees that the set of frequencies corresponding to rotation around the origin is unbounded; indeed, the frequency goes to infinity with the distance to the origin. The first result of this type can be found in the equivalent context of adiabatic theory [3]. Another strand goes back to the question of boundedness of solutions (which is implied by the existence of invariant tori in this low-dimensional situation) [34]. These qualitative results have also been extended to more general mathematical settings [20], [31], [32], [35], [45], [46], [66].

A typical system of this type exhibits a phase space divided into two clearly distinct regions. See Figures 1 to 3, which show numerical experiments in the present setting.

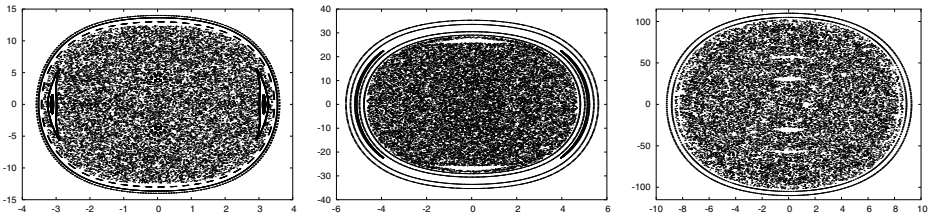

(a) (b) (c)

Fig. 2. Continuation of Figure 1. Phase portraits of the Poincaré map P for (a) $V_1 = 10$, (b) $V_1 = 25$, and (c) $V_1 = 100$.

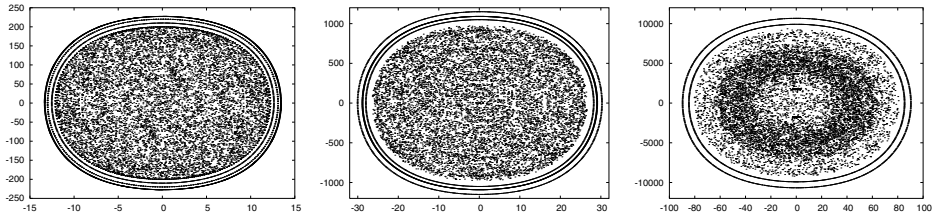

(a) (b) (c)

Fig. 3. Continuation of Figure 2. Phase portraits of the Poincaré map P for (a) $V_1 = 200$, (b) $V_1 = 1{,}000$, and (c) $V_1 = 10{,}000$.

One region, bounded away from the origin, consists largely of invariant tori, with small layers of chaotic dynamics between them. Indeed, one can show that the measure of these layers vanishes exponentially fast as the distance to the origin goes to infinity [47], [8]. The other region has mainly chaotic dynamics. In this paper, we employ a quantitative existence result [15] to obtain bounds on the locations and frequencies of invariant tori.

2. Physical Background

At low temperatures, particles in a dilute boson gas can reside in the same quantum (ground) state, forming a Bose-Einstein condensate (BEC) [17]. This was first observed experimentally in 1995 with vapors of rubidium and sodium [2], [18]. In these experiments, atoms were confined in magnetic traps, evaporatively cooled to temperatures of a few hundred nanokelvin, left to expand by switching off the confining trap, and subsequently imaged with optical methods [17]. A sharp peak in the velocity distribution was observed below a critical temperature, indicating that condensation had occurred. BECs are inhomogeneous, allowing condensation to be observed in both momentum and position space. The number of condensed atoms N ranges from several thousand to tens of millions.

A BEC has two characteristic length scales: the harmonic oscillator length $a_{ho} = \sqrt{\hbar/[m\omega_{ho}]}$ (which is about a few microns), where $\omega_{ho} = (\omega_x\omega_y\omega_z)^{1/3}$ is the geometric mean of the trapping frequencies, and the mean healing length $\chi = 1/\sqrt{8\pi|a|\bar{n}}$ (which is also about a few microns), where $\bar{n}$ is the mean density and a, the (two-body) s-wave scattering length, is determined by the atomic species of the condensate. Interactions between atoms are repulsive when $a > 0$ and attractive when $a < 0$. For a dilute ideal gas, $a \approx 0$. The length scales in BECs should be contrasted with those in systems like superfluid helium, in which the effects of inhomogeneity occur on a microscopic scale fixed by the interatomic distance [17].

When considering only two-body interactions, the BEC wave function ("order parameter") $\Psi(\vec{r}, t)$ satisfies the Gross-Pitaevskii (GP) equation,

$$i\hbar\Psi_t = \left(-\frac{\hbar^2\nabla^2}{2m} + g_0|\Psi|^2 + \mathcal{V}(\vec{r})\right)\Psi, \tag{1}$$

where $\Psi = \Psi(\vec{r}, t)$ is the condensate wave function, $\mathcal{V}(\vec{r})$ is the external potential, and

the effective interaction constant is $g_0 = [4\pi\hbar^2 a/m][1 + O(\zeta^2)]$, where $\zeta \equiv \sqrt{|\Psi|^2|a|^3}$ is the dilute-gas parameter [17], [33]. A BEC is modeled in the quasi-one-dimensional (quasi-1D) regime when its transverse dimensions are on the order of its healing length and its longitudinal dimension is much larger than its transverse ones [10], [17]. In the quasi-1D regime, one employs the 1D limit of a 3D mean-field theory rather than a true 1D mean-field theory, which would be appropriate were the transverse dimension on the order of the atomic interaction length or the atomic size. The resulting 1D equation is [17], [60]

$$i\hbar\psi_t = -\frac{\hbar^2}{2m}\psi_{xx} + g|\psi|^2\psi + V(x)\psi, \tag{2}$$

where ψ, g, and V are, respectively, the rescaled 1D wave function, interaction constant, and external trapping potential. The quantity $|\psi|^2$ gives the atomic number density. The self-interaction parameter g is tunable (even its sign), because the scattering length a can be adjusted using magnetic fields in the vicinity of a Feshbach resonance [21], [30].

Potentials $V(x)$ of interest include harmonic traps, periodic lattices and superlattices (i.e., optical lattices with two or more wave numbers), and periodically perturbed harmonic traps. The existence of quasi-1D cylindrical ("cigar-shaped") BECs motivates the study of periodic potentials without a confining trap along the dimension of the periodic lattice [37]. Experimentalists use a weak harmonic trap on top of the periodic lattice or superlattice to prevent the particles from spilling out. To achieve condensation, the lattice is typically turned on after the trap. If one wishes to include the trap in theoretical analyses, $V(x)$ is modeled by

$$V(x) = V_1\cos(\kappa_1 x) + V_2\cos(\kappa_2 x) + V_h x^2, \tag{3}$$

where κ_1 is the primary lattice wave number, $\kappa_2 > \kappa_1$ is the secondary lattice wave number, V_1 and V_2 are the associated lattice amplitudes, and V_h represents the magnitude of the harmonic trap. (Note that V_1, V_2, V_h, κ_1, and κ_2 can all be tuned experimentally.) When $V_h \ll V_1, V_2$, the potential is dominated by its periodic contributions for many periods. BECs in optical lattices with up to 200 wells have been created experimentally [50].

In this work, we let $V_h = 0$ and focus on periodic lattices and superlattices. Spatially periodic potentials have been employed in numerous experimental studies of BECs (see, for example, [1], [26]) and have also been studied theoretically (see, for example, [10], [12], [38], [65]). In recent experiments, BECs have also been loaded successfully into superlattices with $\kappa_2 = 3\kappa_1$ [51]. Additionally, over the past couple years, there has been an increasing number of theoretical studies on BECs in superlattices [16], [22], [36], [54], [55].

As mentioned in Section 1.1 and proven below, we obtain bounds on the locations and frequencies of invariant tori. Our paper establishes quasiperiodic dynamics for sufficiently large amplitude. By a slight adaptation of the argument (see Remark 10 below), it can be shown that the quasiperiodic dynamics has large measure at large amplitude. It is generally conjectured that chaotic dynamics exist where invariant tori have been destroyed. In the present model, the presence of chaos (which was studied in BECs in, e.g., [12], [14], [16], [62]) would reflect an irregular spatial profile $R(x)$ (where $|R(x)| = |\psi(x,t)|$ is the amplitude of the BEC wave function), whereas invariant tori correspond to regular (i.e., quasiperiodic) spatial profiles.

Remark 1. When the optical lattice has deep wells (large $|V_1|$ or $|V_2|$), one can also obtain an analytical description of BECs in terms of Wannier wave functions using the so-called tight-binding approximation [42]. In this regime, the BEC dynamics is governed by a discrete nonlinear Schrödinger equation, which is derived by expanding the field operator in a Wannier basis of localized wave functions at each lattice site.

Coherent structure solutions are described with the ansatz

$$\psi(x,t) = R(x)\exp\left(i\left[\theta(x) - \mu t\right]\right), \tag{4}$$

where $R \in \mathbb{R}$ gives the amplitude dynamics of the wave function, θ gives the phase dynamics, and the "chemical potential" μ, defined as the energy it takes to add one more particle to the system, is proportional to the number of atoms trapped in the condensate. When the (temporally periodic) coherent structure (4) is also spatially periodic, it is called a *modulated amplitude wave* (MAW) [53].

Remark 2. The present work is concerned with the spatial amplitude dynamics of solutions of the form (4). To ensure that such solutions are physically relevant, it is important to examine their stability with respect to the dynamics of the GP equation (2). Bronski and coauthors [9], [10], [11] were able to obtain rigorous stability results in some situations using elliptic-function potentials. (For repulsive condensates, for example, they used the ansatz (4) to construct elliptic-function solutions to (2), whose linear stability they proved for $R(x) > 0$ by showing that they were ground states of the GP equation.) Their results can be applied to trigonometric potentials by taking the limit as the elliptic modulus approaches zero. More generally, one can address the stability of solutions of the form (4) through direct numerical simulations of (2) using such solutions as initial wave functions: $\psi(x,0) = R(x)$. It was shown previously, using both lattice and superlattice potentials $V(x)$, that one can obtain numerically stable MAWs for (2) with solutions of the form (4) with trivial phase $\theta = 0$ [54], [56]. Furthermore, the numerically stable "period-doubled" solutions (whose spatial periodicity is twice that of the optical lattice potential) constructed via subharmonic resonances using the ansatz (4) with trivial phase ($\theta = 0$) have very recently been observed experimentally [23].

Inserting (4) into the GP equation (2) and equating real and imaginary parts, one obtains

$$\begin{aligned} \hbar\mu R(x) &= -\frac{\hbar^2}{2m}R''(x) + \left[\frac{\hbar^2}{2m}\left[\theta'(x)\right]^2 + gR^2(x) + V(x)\right]R(x), \qquad (5)\\ 0 &= \frac{\hbar^2}{2m}\left[2\theta'(x)R'(x) + \theta''(x)R(x)\right], \end{aligned}$$

which gives the following nonlinear ordinary differential equation:

$$R'' = \frac{c^2}{R^3} - \frac{2m\mu R}{\hbar} + \frac{2mg}{\hbar^2}R^3 + \frac{2m}{\hbar^2}V(x)R. \tag{6}$$

The parameter c is defined via the relation

$$\theta'(x) = \frac{c}{R^2(x)}, \tag{7}$$

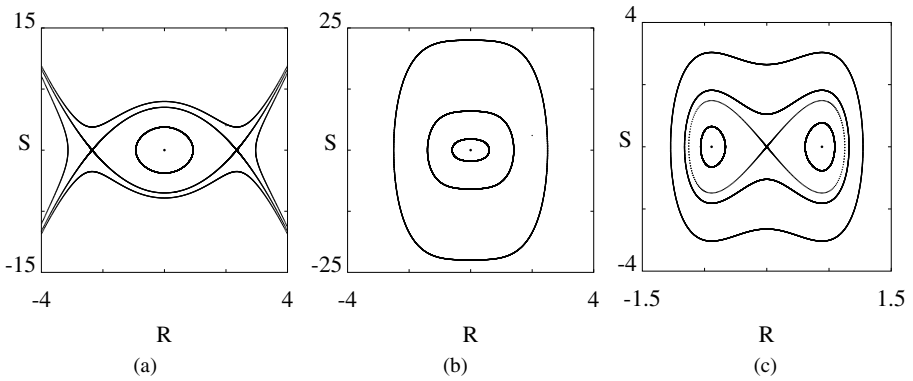

Fig. 4. Phase portraits of coherent structures in BECs with no external potential. The signs of μ and g determine the dynamics of (8). (a) Repulsive BEC with $\mu > 0$. Orbits inside the separatrix have bounded amplitude $|R(x)|$. The period of such orbits increases as one approaches the separatrix. In this case, the dynamical system can be rescaled so that $R'' = -R + R^3$. (b) Attractive BEC with $\mu > 0$. The dynamical system can be rescaled so that $R'' = -R - R^3$. (c) Attractive BEC with $\mu < 0$. Here there are two separatrices, each of which encloses periodic orbits satisfying $R \neq 0$. The dynamical system can be rescaled so that $R'' = R - R^3$.

which plays the role of conservation of "angular momentum," as discussed by Bronski and coauthors [10]. Constant phase solutions (i.e., standing waves) constitute an important special case and satisfy $c = 0$. In the rest of the paper, we consider only standing waves, so that

$$R'' = -\frac{2m\mu R}{\hbar} + \frac{2mg}{\hbar^2}R^3 + \frac{2m}{\hbar^2}V(x)R. \tag{8}$$

Remark 3. When $V(x) \equiv 0$, the dynamical system (8) is the autonomous, integrable Duffing oscillator. Its qualitative dynamics in the physically relevant situation of bounded $|R|$ is illustrated in Figure 4. The methodology developed in the present paper can handle attractive BECs ($g < 0$) with either $\mu < 0$ or $\mu > 0$ but not repulsive BECs, as equation (8) has unbounded solutions when $g > 0$.

3. Main Result

This section states the main theorem of this paper, which concerns the existence of quasiperiodic dynamics in a class of systems of the form (8), including the cases with $V(x)$ given by periodic lattices and superlattices. Applications to these cases are subsequently given in two subsections.

The equation of motion (8) describes a $1\frac{1}{2}$-degree-of-freedom Hamiltonian system whose forcing is periodic. We will allow arbitrary analytic periodic potential functions V. We first rescale the period of the forcing to 1. We introduce the phase variable $\xi = T^{-1}x \pmod 1$, where $T > 0$ is the minimal period of V. Letting $'$ denote differentiation

with respect to ξ, we define $S = R'$, and

$$z_2(\xi) = T^2\left(\frac{m\mu}{\hbar} - \frac{m}{\hbar^2}V(x)\right), \qquad z_4 = -T^2\frac{mg}{2\hbar^2}, \qquad U(R,\xi) = z_2(\xi)R^2 + z_4R^4.$$

This gives the suspended dynamical system

$$\begin{aligned} R' &= S, \\ S' &= -\frac{\partial U}{\partial R}(R,\xi), \\ \xi' &= 1, \end{aligned} \tag{9}$$

with Hamiltonian

$$H(R,S,\xi) = \frac{1}{2}S^2 + U(R,\xi). \tag{10}$$

Remark 4. We restrict to analytic systems for convenience only. It is not a necessary restriction, as our result is based on Herman's *translated curve theorem* [27], [28], which requires only C^4 smoothness. Furthermore, finite-smoothness KAM results can be obtained from analytic ones by inverse approximation [58]. The restriction to analytic systems allows one to use Cauchy's integral theorem to replace C^k norms by C^0 ones.

Remark 5. Because $z_4 > 0$, the function U is a well; that is, $U \to +\infty$ as $R \to \pm\infty$ for all ξ. It is even in R, which has important ramifications for the sizes of the perturbations in our subsequent analysis. (See, for example, Lemma 16 below, where the leading term in the nonintegrable parts F_1 and F_2 would have been order one instead of going to zero as $R \to +\infty$ were it not for this symmetry.)

We introduce action-angle coordinates as follows. (The details are in Section 4.) Let $H_0(R,S) = \frac{1}{2}S^2 + z_4R^4$. For $h > 0$, define the action $I = I(h)$ to be the area in the (R,S)-plane enclosed by the curve $H_0(R,S) = h$. Let the angle $\phi = \phi(R,S) \in \mathbb{R}/\mathbb{Z}$ be such that the transformation $(R,S) \mapsto (\phi, I)$ is symplectic. This defines ϕ uniquely if we set $\phi(0,S) \equiv 0$ for $S > 0$.

In action-angle coordinates, the Hamiltonian takes the form $K(\phi, I, \xi) = K_0(I) + K_1(\phi, I, \xi)$, where $K_0(I) = H_0(R,S)$. We consider K as a perturbation of K_0. For any $I_0 > 0$, the unperturbed system K_0 has an invariant torus $I = I_0$ with frequency $\omega = K_0'(I_0)$ in ϕ. We say that this frequency is of *constant type* with parameter $\gamma > 0$ if

$$\left|\omega - \frac{p}{q}\right| \geq \gamma q^{-2} \quad \text{for all} \quad \frac{p}{q} \in \mathbb{Q}. \tag{11}$$

This is a special type of Diophantine condition [27], [28].

For a function f defined on a set $\mathcal{D}$, we define $\|f\|_{\mathcal{D}} = \sup_{\mathcal{D}} |f|$. If f is vector-valued, then $\|f\|_{\mathcal{D}}$ is the maximum of the norms of the components. For $d > 0$, let $\bar{\mathcal{D}}(d) = \{\xi \in \mathbb{C}/\mathbb{Z}\colon\ |\operatorname{Im}(\xi)| \leq 2d\}$.

With the additional notation $\eta = 18\gamma$, $M = z_4I_0$, $c = 126/25 = 5.04$, and $b_1 = \int_0^1 (1-u^4)^{1/2}\,\mathrm{d}u = 0.874019\ldots$, the main result of this paper can now be stated as follows.

Theorem 6. *The Hamiltonian K has an invariant torus with frequency $\omega = K_0'(I_0)$ in ϕ if there exist ν, γ, $d > 0$, and $b_2 > 0$ with $0 \le \nu \le \frac{1}{9} \cdot 2^{-7/3}$ and $0 < \gamma \le \frac{49}{72}$ such that ω is of constant type with parameter γ and the following conditions hold:*

$$A\left(1 + \frac{3\log B}{\log M}\right) \le 2^{-4/3} b_1^{-4/3} \log(2), \tag{12}$$

$$1 < M, \tag{13}$$

$$L \le \frac{47}{200}, \tag{14}$$

$$b_2 \le 18[1 + 24b_1(\eta + 2d)](1 + L)^{2/3}(1 - L)^{1/3} \log(M), \tag{15}$$

$$2 \le BM^{1/3}, \tag{16}$$

$$\|z_2\|_{\bar{\mathcal{D}}(d)} \le \delta \frac{M^{2/3}}{\log^2(M)}, \tag{17}$$

where

$$\begin{aligned}
L &= 2^{4/3} \cdot 3b_1^{4/3}\eta M^{-1/3} + \frac{2b_2 d}{\log(M)},\\
A &= \frac{1 + 4(\eta + 2d)}{d} \max\left\{ \frac{2\eta}{3} M^{-1/3}\log(M) + \left(\frac{2^{2/3}}{9} + \frac{7\nu}{2}\right) d b_1^{-4/3} b_2 \right.\\
&\qquad + \frac{2^{-1/3}}{27} b_1^{-4/3}(1 - L)^{-5/3} L^2 \log(M), 2M^{-1/3}\log(M)\\
&\qquad \left. + \frac{3\nu}{2} d b_1^{-4/3} b_2 \right\},\\
B &= 2^{-13/3} 3^3 7^8 c^{-1} d b_1^{-4/3} b_2 \eta^{-6} \left(\frac{1}{\log(M)} + \frac{2^{-7/3}}{3} b_1^{-4/3} b_2 \frac{M^{1/3}}{\log^2(M)} \right),\\
\delta &= \frac{2^{-1/3}}{3} \nu d b_2^2 b_1^{-5/3}(1 + L)^{-2/3}[1 + 24b_1(\eta + 2d)]^{-3}.
\end{aligned}$$

The torus lies in the region given by $|I - I_0| \le b_2 I_0 [\log(z_4 I_0)]^{-1}(\frac{11}{19} d + \rho)$.

Remark 7. Conditions (12)–(16) are satisfied for M sufficiently large, while (17) is a restriction on z_2 and hence on V. The theorem implies that $\|z_2\|_{\bar{D}(d)}$ can be taken roughly proportional to $z_4^{2/3} I_0^{2/3}$. Equation (24) below shows that $z_4^{-1/6} I_0^{1/3}$ is proportional to the maximal R coordinate $R_{\max}$ on the torus $H_0(R, S) = K_0(I_0)$, so $\|z_2\|_{\bar{D}(d)}$ is roughly proportional to $z_4 R_{\max}^2$. This fits with the numerically computed phase portraits in Figures 1 to 3.

In terms of physical parameters, this implies that for an attractive BEC with given scattering length $a < 0$ and chemical potential μ loaded into an arbitrary periodic lattice of amplitude $\|V\|$ (with any number of wave numbers), the wave function's spatial component $R(x)$ is quasiperiodic with two frequencies if its maximum $R_{\max}$ is large enough, its frequencies satisfy the Diophantine condition (11), and the amplitude $\|V\|$

of the lattice potential is sufficiently small. The lower bound on $R_{\max}$ scales as $\kappa/\sqrt{|a|}$, where $\kappa = 2\pi/T$ is the lattice amplitude (and we recall that a is the two-body scattering length and T is the minimal period of the lattice), whereas the upper bound on $\|V\|$ scales as $aR_{\max}^2$. All frequency ratios that are algebraic numbers of index 2 satisfy the Diophantine condition (for some $\gamma > 0$).

Remark 8. The conditions of the theorem imply that M should be larger than roughly 10^6. Indeed, from $A \geq 8 \cdot 2M^{-1/3}\log(M)$ and $BM^{1/3} \geq 2$, it follows that $A[1 + 3\log(B)/\log(M)] \geq 48M^{-1/3}\log(2)$. Hence, condition (12) implies that $M \geq 2^{16}3^3b_1^4 \approx 10^6$.

As an illustration, we choose M and the parameters b_2, γ, d, ν based on a numerical experiment where we evaluate the conditions of the theorem on a Cartesian grid of $360 \times 180 \times 120 \times 120 \times 20$ points in the cube $[10^6, 10^{18}] \times [10^{-6}, 1] \times [10^{-3}, 10] \times [10^{-3}, 10] \times [10^{-3}, \frac{1}{9} \cdot 2^{-7/3}]$ in (M, b_2, γ, d, ν) space, taking a logarithmic scale in the first four components and a linear scale in the last. For each M, we compute the largest value of the coefficient δ over all grid points where all the conditions hold in order to obtain a good choice of parameter values. Figure 5 shows the largest δ one can obtain for a range of M.

Corollary 9. *If K has an invariant torus with frequency $K_0'(I_0)$, then the return map of K on the surface of section $\xi = 0$ has an Aubry-Mather set with rotation number ω for any $\omega > K_0'(I_0)$.*

The corollary follows immediately from Aubry-Mather theory [4], [40], [44] and the monotonicity of K_0'. Indeed, the Poincaré map P_0 corresponding to K_0 is given by

$$P_0\colon (\phi, I) \mapsto (\phi + K_0'(I), I).$$

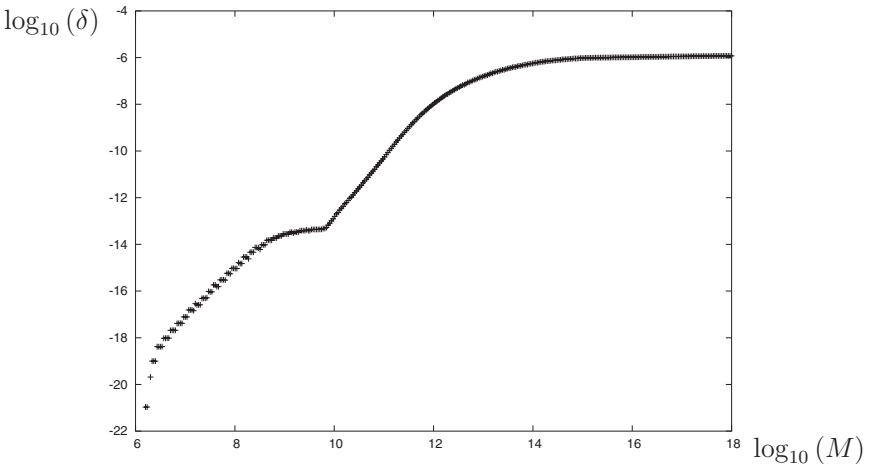

Fig. 5. Log-log plot of M versus the largest value of δ found by a numerical computation.

From the monotonicity of K_0', it follows that this is a twist map. The proof of the main result of [15] shows that the Poincaré map P corresponding to K also satisfies the twist condition. Alternatively, this also follows directly from the fact that the function U is superquadratic.

Remark 10. The translated curve theorem used (in [15]) to prove Theorem 6 shows persistence of invariant tori under relatively large perturbations (compared to other KAM or twist theorems), at the expense of excluding all but the "most quasiperiodic" frequencies ω. If the Diophantine condition is relaxed to include a nonzero measure of frequencies, then one can similarly show that the region outside the innermost invariant torus contains a set of invariant tori of positive measure, where the measure converges exponentially fast to full measure as $I \to +\infty$. The remaining dynamics in this region is presumably chaotic, but due to the low dimension of the system, there cannot be any Arnol'd diffusion. Thus, it is at worst bounded chaos. Among many papers on this subject, see, e.g., [8], [47], [58] for further details.

By contrast, the region on the inside seems to exhibit chaotic dynamics, as can be seen in Figures 1 to 3. In the near-autonomous setting (i.e., for small-amplitude V), the figures show large domains of integrable dynamics in the interior region. A perturbation analysis for a similar system shows that, as the amplitude of V goes to infinity, the sizes of these islands vanish. However, their number increases reciprocally, so an integrable set of measure $O(1)$ remains [48].

In the next two sections, we consider potentials $V(x)$ with one and two wave numbers. The former case describes BECs in periodic lattices [10], [12], [38], [52], [53], and the latter case, which is now experimentally accessible [51], describes BECs in periodic superlattices [22], [36], [54].

3.1. Example 1: BECs in Periodic Lattices

Optical lattice potentials are created experimentally as interference patterns of counterpropagating laser beams [19]. In the periodic case, the external potential is typically taken to be sinusoidal,

$$V(x) = -V_1 \cos(\kappa x), \tag{18}$$

where $\kappa = 2\pi/T$ is the lattice wave number.

We write equation (8) in the form

$$\begin{aligned} R' &= S, \\ S' &= -\alpha_1 R + \alpha_3 R^3 + V_1 R \cos(\kappa x), \\ x' &= 1, \end{aligned} \tag{19}$$

where $\alpha_1 \propto \mu$, $\alpha_3 \propto g$, and $'$ denotes differentiation with respect to x. The parameters $V_1, \alpha_1, \alpha_3 \in \mathbb{R}$, and $\kappa > 0$ can all be adjusted experimentally. The phase variables are $(R, S) \in \mathbb{R}^2$ and $x \in \mathbb{R}/(2\pi\kappa^{-1}\mathbb{Z})$. The associated Poincaré map P, which is defined to be the first return map on the section $x = 0$, corresponds to the flow over $2\pi\kappa^{-1}$.

Equation (19) has two reversible symmetries:

$$(R, S, x) \mapsto (-R, S, -x), \qquad (R, S, x) \mapsto (R, -S, -x).$$

The map P is thus reversible under reflection in both coordinate axes,

$$R_j \circ P \circ R_j = P^{-1}, \quad j = 1, 2,$$

where R_1 and R_2 are the reflections with respect to the axes.

Additionally, (19) is invariant under two rescalings:

$$(R, S, x; \alpha_1, \alpha_3, \kappa, V_1) \mapsto (R, \lambda S, \lambda^{-1}x; \lambda^2\alpha_1, \lambda^2\alpha_3, \lambda\kappa, \lambda^2 V_1), \tag{20}$$

$$(R, S, x; \alpha_1, \alpha_3, \kappa, V_1) \mapsto (\mu R, \mu S, x; \alpha_1, \mu^{-2}\alpha_3, \kappa, V_1). \tag{21}$$

The corresponding invariants for the Poincaré map are obtained by dropping the x components.

One can rescale (19) using these invariants to reduce to the cases where $\alpha_1 = 0, \pm 1$ and $\alpha_3 = 0, \pm 1$. We look in detail at the case $\alpha_1 = -1$, $\alpha_3 = -1$, corresponding to an attractive BEC with a negative chemical potential, where the underlying integrable system (with $V_1 = 0$) is a "figure eight" (consisting of a central saddle point and two exterior centers, as shown in Figure 4c).

Because of the second rescaling (21), the parameter α_3 simply measures the size of phase space. The first rescaling (20) shows that decreasing κ increases the nonintegrable perturbation by a square law. Intuitively, a large lattice wave number κ implies that the Poincaré map corresponds to short-"time" integration in x and is thus "near" the vector field. With κ rescaled to 1, as was done in stating and proving our main result, the perturbation $V(x)$ in (19) has unit period.

Figures 1 to 3 show phase portraits of P at several amplitudes of the potential for $(\alpha_1, \alpha_3, \kappa) = (-1, -1, 1)$. One obtains qualitatively similar results for other values of the lattice depth V_1 if the wave number κ is rescaled, as indicated above. As remarked previously, the phase space in these phase portraits is divided into two clearly distinct regions: an outer one in which the dynamics consists in large measure of invariant circles and Cantor-like Aubry-Mather sets (that wind around the origin at large distance) and an inner one in which the dynamics is mostly chaotic. Our numerical simulations, which show the same scaling that our theoretical results indicate, suggest the presence of (parameter-dependent) integrable dynamics of positive but small measure inside the "chaotic sea" [48].

Remark 11. A similar combination of islands of invariant tori within a chaotic sea occurs in the example of a parametrically forced planar pendulum [7]. The division of phase space into a mostly quasiperiodic and a mostly chaotic region is the typical behavior that one expects to observe in a large class of forced one-degree-of-freedom Hamiltonian systems [15].

Applying Theorem 6 for $V(x)$ given by (18) implies that the system (19) has an invariant torus with frequency vector $(\omega, 1)$ provided ω satisfies the conditions of Theorem 6.

The R-amplitude is roughly equal to $R_{\max}$, given by [see equation (24) and Lemma 13]

$$R_{\max} = 3b_1 \frac{\hbar\kappa\omega}{\pi\sqrt{-mg}},$$

where $g < 0$ for the present case of attractive BECs.

3.2. Example 2: BECs in Periodic Superlattices

Optical superlattices consist of small-scale lattices subjected to a long-scale periodic modulation. In recent experiments, BECs were created in superlattice potentials with a wave number ratio of 1:3 [51]. However, theoretical research concerning BECs in superlattices has only begun to gain prevalence [22], [36], [54].

To consider the case of (symmetric) periodic superlattices, we examine the potential

$$V(x) = -\left[V_1 \cos(\kappa_1 x) + V_2 \cos(\kappa_2 x)\right], \tag{22}$$

where $\kappa_2 > \kappa_1$ without loss of generality and $\kappa_2/\kappa_1 \in \mathbb{Q}$. The minimal period is $T = 2\pi/\kappa$, where $\kappa := \gcd(\kappa_1, \kappa_2)$.

Equation (8) is then written

$$\begin{aligned} \frac{dR}{dx} &= S, \\ \frac{dS}{dx} &= -\alpha_1 R + \alpha_3 R^3 + V_1 R\cos(\kappa_1 x) + V_2 R\cos(\kappa_2 x), \\ \frac{dx}{dx} &= 1, \end{aligned} \tag{23}$$

where all the parameters are again experimentally adjustable.

Applying Theorem 6 for $V(x)$ given by (22) with $\kappa_2/\kappa_1 \in \mathbb{Q}$ (i.e., for periodic superlattices) implies that (23) has an invariant torus with frequency vector $(\omega, 1)$ provided ω satisfies the conditions of Theorem 6. As in the regular lattice case, the R-amplitude is roughly equal to $R_{\max}$, where

$$R_{\max} = 3b_1 \frac{\hbar\kappa\omega}{\pi\sqrt{-mg}},$$

and we recall that $2\pi/\kappa$ is the period of $V(x)$ and $g < 0$ for attractive BECs.

Remark 12. If κ_2/κ_1 is not rational, then the potential V is not periodic. If κ_1 and κ_2 satisfy a Diophantine condition, then one can prove the existence of invariant tori at large distance from the origin [32]. We conjecture that it is possible to quantify this existence result analogous to the periodic case [15]. If κ_1 and κ_2 are not Diophantine—for example, if κ_2/κ_1 is a Liouville number—then one expects unbounded solutions and no invariant tori [29].

4. Proof of the Main Result

To prove Theorem 6, we first construct action-angle coordinates explicitly. We then employ the KAM theorem of Chow et al. [15] to complete the proof after a suitable transformation of the action variable.

4.1. The Action and K_0

Define the action by

$$I(h) = \int_{H_0=h} S\,\mathrm{d}R = 4\int_0^{R_{\max}} \sqrt{2h - 2z_4R^4}\,\mathrm{d}R,$$

where $H_0(R, S) = \frac{1}{2}S^2 + z_4R^4$ and $R_{\max} = R_{\max}(h) > 0$ is the solution of $H_0(R_{\max}, 0) = h$; that is, $R_{\max} = z_4^{-1/4}h^{1/4}$. With the substitution $u = R/R_{\max}$ and the relation $h = z_4R_{\max}^4$, the above integral reduces to

$$I(h) = 4\sqrt{2}b_1 z_4^{1/2}R_{\max}^3 = 4\sqrt{2}b_1 z_4^{-1/4}h^{3/4}. \tag{24}$$

Lemma 13. *The unperturbed Hamiltonian in action-angle coordinates is given by*

$$K_0(I) = 2^{-10/3}b_1^{-4/3}z_4^{1/3}I^{4/3}.$$

The proof follows from the calculation above, noting that the unperturbed Hamiltonian K_0 is the inverse of the function I because $H_0(R, S) = K_0(I)$ for $I = I(H_0(R, S))$. The function I is invertible because

$$\frac{\partial I}{\partial h} = 3\sqrt{2}b_1 z_4^{-1/4}h^{-1/4} > 0.$$

Remark 14. One could also define the action to be the area enclosed by the curve $\frac{1}{2}S^2 + \bar{z}_2R^2 + z_4R^4 = h$, where $\bar{z}_2$ is the average of z_2, or even the area enclosed by $H = h$, where ξ is considered as a parameter (that is, $\xi' = 0$ in the unperturbed system). In the latter case, the action and angle will depend on ξ. Although these two approaches each leave a smaller term in the perturbation than our choice, and are therefore theoretically more pleasing, they lead to technical difficulties in the estimates we need to perform, as the expressions for the action and angle will involve elliptic integrals that depend on the phase variables.

4.2. The Angle

In the upper half-plane ($S \geq 0$), we define the angle by

$$\phi(h, R) = \left(\frac{\partial I}{\partial h}\right)^{-1} \int_0^R \frac{1}{\bar{S}(h, w)}\,\mathrm{d}w \pmod 1,$$

where $\bar{S}(h, R) = \sqrt{2h - 2z_4R^4}$ is the positive solution of $H_0(R, \bar{S}(h, R)) = h$. Note that $\frac{\partial I}{\partial h} = \oint_{H_0=h} S^{-1}\,\mathrm{d}R$. A similar definition holds in the lower half-plane, where $\phi =$

$\frac{1}{2} - (\frac{\partial I}{\partial h})^{-1} \int_0^R \bar{S}^{-1}\,\mathrm{d}w \pmod 1$. Henceforth, we restrict to the upper half-plane without loss of generality.

Lemma 15. *The following formulas hold:*

$$\begin{aligned}\phi(h, R) &= \frac{1}{6b_1}\int_0^{R/R_{\max}} (1-u^4)^{-1/2}\,\mathrm{d}u,\\ \bar{S}(h, R)\frac{\partial\phi}{\partial h}(h, R) &= -\frac{\sqrt{2}}{24b_1}h^{-1/2}\frac{R}{R_{\max}}.\end{aligned}$$

Defining $r = r(h, R) = R/R_{\max}(h)$, it follows that ϕ depends only on r:

$$\phi(h, R) = \bar{\phi}(r(h, R)), \quad \text{where } \bar{\phi}(r) = \frac{1}{6b_1}\int_0^r (1-u^4)^{-1/2}\,\mathrm{d}u.$$

In particular, $\bar{\phi}(1) = 1/4$.

Proof. Using the definition of ϕ and the substitution $w = R_{\max}u$, we obtain

$$\begin{aligned}\phi &= \left(\frac{\partial I}{\partial h}\right)^{-1}\frac{1}{\sqrt{2}}z_4^{-1/2}R_{\max}^{-1}\int_0^r (1-u^4)^{-1/2}\,\mathrm{d}u\\ &= \frac{1}{6b_1}z_4^{-1/4}h^{1/4}R_{\max}^{-1}\int_0^r (1-u^4)^{-1/2}\,\mathrm{d}u,\end{aligned}$$

which proves the first formula. Furthermore,

$$\begin{aligned}\bar{S}(h, R)\frac{\partial\phi}{\partial h} &= -(2h - 2z_4R^4)^{1/2}\frac{1}{6b_1}(1-r^4)^{-1/2}RR_{\max}^{-2}\frac{\partial R_{\max}}{\partial h}\\ &= -\frac{\sqrt{2h}}{24b_1}R_{\max}^{-1}z_4^{-1/4}h^{-3/4}r\\ &= -\frac{\sqrt{2}}{24b_1}h^{-1/2}r.\end{aligned}$$

□

4.3. Localization and Rescaling

The system corresponding to K can be computed directly and is given by

$$\begin{aligned}\phi' &= K_0'(I) + f_1(\phi, I, \xi),\\ I' &= f_2(\phi, I, \xi),\\ \xi' &= 1,\end{aligned}$$

where $f_1(\phi, I, \xi) = -S\frac{\partial\phi}{\partial h}\frac{\partial H_1}{\partial R}$ and $f_2(\phi, I, \xi) = -S\frac{\partial I}{\partial h}\frac{\partial H_1}{\partial R}$.

For a fixed I_0, we define a localization transformation $(\phi, I, \xi) \mapsto (\phi, J, \xi)$ by $I = I_0 + \beta(I_0)J$, with $\beta(I_0) = b_2 I_0[\log(z_4 I_0)]^{-1}$, where $b_2 \in \mathbb{R}$ is positive and will be determined later. This takes the unperturbed torus $I = I_0$ to $J = 0$ and rescales the action

variable, so that the components f_1, f_2 of the perturbation are roughly the same size after rescaling and some other conditions are met (see Remark 21 below). Although it is not a symplectic transformation, it nonetheless maps Hamiltonian systems to Hamiltonian systems.

Define $\omega = K_0'(I_0)$ and $m = \beta(I_0)K_0''(I_0)$, so that

$$\omega = \frac{1}{3}\cdot 2^{-4/3}b_1^{-4/3}z_4^{1/3}I_0^{1/3}, \tag{25}$$

$$m = \frac{1}{9}\cdot 2^{-4/3}b_1^{-4/3}b_2\frac{z_4^{1/3}I_0^{1/3}}{\log(z_4I_0)}. \tag{26}$$

Lemma 16. *In (ϕ, J, ξ) coordinates, the system is written*

$$\phi' = \omega + mJ + g(J) + F_1(\phi, J, \xi), \quad J' = F_2(\phi, J, \xi), \quad \xi' = 1,$$

where, for some J_*, $J^* \in (0, J)$,

$$\begin{aligned}
g(J) &= \frac{1}{2}\beta(I_0)^2K_0'''(I_0+\beta(I_0)J_*)J^2 \\
&= -\frac{1}{27}\cdot 2^{-4/3}b_1^{-4/3}z_4^{1/3}I_0^{1/3}\left(1+\frac{b_2J_*}{\log(z_4I_0)}\right)^{-5/3}\left(\frac{b_2J}{\log(z_4I_0)}\right)^2, \\
\frac{\partial g}{\partial J}(J) &= \beta(I_0)^2K_0'''(I_0+\beta(I_0)J^*)J \\
&= -\frac{1}{27}\cdot 2^{-1/3}b_1^{-4/3}b_2\frac{z_4^{1/3}I_0^{1/3}}{\log(z_4I_0)}\left(1+\frac{b_2J^*}{\log(z_4I_0)}\right)^{-5/3}\frac{b_2J}{\log(z_4I_0)}, \\
F_1(\phi, J, \xi) &= f_1(\phi, I_0+\beta(I_0)J, \xi) \\
&= \frac{1}{3}\cdot 2^{-2/3}b_1^{-2/3}z_2(\xi)r^2z_4^{-1/3}I_0^{-1/3}\left(1+\frac{b_2J}{\log(z_4I_0)}\right)^{-1/3}, \\
F_2(\phi, J, \xi) &= \beta(I_0)^{-1}f_2(\phi, I_0+\beta(I_0)J, \xi) \\
&= -3\cdot 2^{1/3}b_1^{1/3}z_2(\xi)r(1-r^4)^{1/2}b_2^{-1}\frac{\log(z_4I_0)}{z_4^{1/3}I_0^{1/3}}\left(1+\frac{b_2J}{\log(z_4I_0)}\right)^{2/3}.
\end{aligned}$$

The lemma shows that the nonintegrable parts F_1 and F_2 are order $I_0^{-1/3}$ in the leading term; this would have been order 1 had the original function U included a cubic term.

Proof. Write $\Omega(J) = K_0'(I_0+\beta(I_0)J)$, so that $\omega = \Omega(0)$ and $m = \Omega'(0)$. By Taylor's theorem,

$$g(J) = \Omega(J) - \omega - mJ = \frac{1}{2}\Omega''(J_*)J^2, \qquad g'(J) = \Omega'(J) - m = \Omega''(J^*)J.$$

Furthermore, $\beta(I_0)J' = I'$. The expressions for g, g', F_1, and F_2 follow by direct calculation from (24) and Lemma 15. □

4.4. Proof of Theorem 6

The rescaled system is a perturbation of $\phi' = \omega + mJ + g(J)$, $J' = 0$. The unperturbed system has an invariant torus $J = 0$ with ϕ-frequency ω. Assume that ω is of constant type with parameter $\gamma > 0$. We now study the persistence of this torus under the perturbation $F = (F_1, F_2)$.

For $d > 0$, $\eta = 18\gamma$, and $\rho = (3m)^{-1}\eta$, we define a (complex) neighborhood $\mathcal{D}_0$ of the unperturbed torus by

$$\mathcal{D}_0 = \mathcal{D}_0(\eta, \rho, d) = \{(\phi, J, \xi) \in \mathbb{C}/\mathbb{Z} \times \mathbb{C} \times \mathbb{R}/\mathbb{Z}\colon\ |\operatorname{Im}(\phi)| \le \eta, |J| < \rho\} + 2d.$$

The KAM theorem of Chow et al. [15] now shows that the perturbed system has an invariant torus with frequency ω satisfying $|J| \le \frac{11}{19}d + \rho$ provided

$$\left\| \frac{\partial g}{\partial J} \right\|_{\mathcal{D}_0} < m/4, \tag{27}$$

$$\omega_0 \le \omega. \tag{28}$$

The first of these conditions is a twist condition, and the second states that the perturbation is small enough, where ω_0 is defined as follows. Let $c = 5.04$, and $\|F\|_{\mathcal{D}_0} = \max\{\|F_1\|_{\mathcal{D}_0}, \|F_2\|_{\mathcal{D}_0}\}$. Let L_W denote the Lambert W function (i.e., the inverse of $W \mapsto We^W$). Then,

$$\begin{aligned}
\omega_0 &= \alpha_0 \max\left\{1, \frac{1}{\log 2} L_W(b \log 2)\right\},\\
b &= \frac{2+3m}{c\gamma^2} \max\left\{12, \frac{7^8}{108(\eta - 6\gamma)^4}\right\} \max\{md, 2\|F\|_{\mathcal{D}_0}\},\\
\alpha_0 &= \frac{3 + 12(\eta + 2d)}{2d}\left(\|F\|_{\mathcal{D}_0} + 2C \max\left\{1, \frac{2\|F\|_{\mathcal{D}_0}}{md}\right\}\right),\\
C &= \frac{2}{3}\max\{m(2d+\rho) + \|g\|_{\mathcal{D}_0} + \|F\|_{\mathcal{D}_0}, 1\}.
\end{aligned} \tag{29}$$

Lemmas 17–20 show that the twist and smallness conditions follow from conditions (12)–(17) of Theorem 6.

Lemma 17. *Condition (27) follows from (14).*

Proof. For $|J| \le \rho + 2d$, it follows that

$$\left\| \frac{b_2 J}{\log(M)} \right\|_{\mathcal{D}_0} \le b_2 \frac{\rho + 2d}{\log(M)} = L \le \frac{47}{200}.$$

Hence, for J^* as in Lemma 16,

$$\left\| \left(1 + \frac{b_2 J^*}{\log(M)}\right)^{-5/3} \frac{b_2 J}{\log(M)} \right\|_{\mathcal{D}_0} \le \left(1 - \frac{47}{200}\right)^{-5/3} \frac{47}{200} < \frac{3}{8}.$$

The desired result now follows from Lemma 16. □

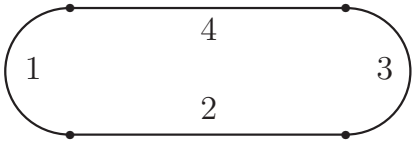

Fig. 6. The set $\mathcal{E}$, with labels for the four parts of its boundary (two semicircles and two line segments).

Lemma 18. *Let $r = R/R_{\max}$, as before. Then,*

$$\|r\|_{\mathcal{D}_0} \leq 1 + 24b_1(\eta + 2d),$$
$$\|r(1 - r^4)^{1/2}\|_{\mathcal{D}_0} \leq [1 + 24b_1(\eta + 2d)]^3.$$

Proof. Without loss of generality, we restrict to ϕ satisfying $\mathrm{Re}(\phi) \in [0, \frac{1}{4}]$ (mod 1). Observe that $|\operatorname{Im}\phi| \leq \eta + 2d$ in $\mathcal{D}_0$. Thus, we can consider $\phi \in \bar{\mathcal{D}} = \{\phi \in \mathbb{C}/\mathbb{Z}\colon \mathrm{Re}(\phi) \in [0, \frac{1}{4}](\mathrm{mod}\ 1), |\operatorname{Im}\phi| \leq \eta + 2d\}$.

Let $\mathcal{E}(\varepsilon) = [0, 1] + \varepsilon \subset \mathbb{C}$. It is obvious that r will be in $\mathcal{E}$ for large enough ε. Let ε be the smallest number such that $r = r(\phi) \in \mathcal{E} = \mathcal{E}(\varepsilon)$ for all $\phi \in \bar{\mathcal{D}}$. Hence, there exists $\phi_0 \in \bar{\mathcal{D}}$ such that $r(\phi_0)$ is on the boundary of $\mathcal{E}$. Furthermore, $r(\mathrm{Re}(\phi_0)) \in [0, 1]$. Therefore, by the mean value theorem,

$$\varepsilon \leq |r(\phi_0) - r(\mathrm{Re}(\phi_0))| \leq \left\| \frac{\partial r}{\partial \phi} \right\|_{\bar{\mathcal{D}}} (\eta + 2d).$$

By definition, $\frac{\partial \phi}{\partial r}(r) = (6b_1)^{-1}(1 - r^4)^{-1/2}$. Thus,

$$\frac{\partial r}{\partial \phi}(\phi) = 6b_1(1 - r^4)^{1/2}.$$

We will now show that $\|1 - r^4\|_{\mathcal{E}} \leq (1 + \varepsilon)^4$. By the maximum modulus theorem, $\|1 - r^4\|_{\mathcal{E}}$ is attained on the boundary of $\mathcal{E}$, which looks like a stadium and consists of four parts (see Figure 6). Part 1 is parametrized by $r = \varepsilon \exp(i\theta)$, where $\theta \in [\pi/2, 3\pi/2]$. Hence, $|1 - r^4| \leq 1 + \varepsilon^4 \leq (1 + \varepsilon)^4$. Part 2 is parametrized by $r = u - \varepsilon i$, with $u \in [0, 1]$. Consequently, $|1 - r^4| \leq 1 - u^4 + 4u^3\varepsilon + 6u^2\varepsilon^2 + 4u\varepsilon^3 + \varepsilon^4 \leq 1 + 4\varepsilon + 6\varepsilon^2 + 4\varepsilon^3 + \varepsilon^4 \leq (1 + \varepsilon)^4$. Part 3 is parametrized by $r = 1 + \varepsilon \exp(i\theta)$, where $\theta \in [-\pi/2, \pi/2]$. Hence, $|1 - r^4| \leq 4\varepsilon + 6\varepsilon^2 + 4\varepsilon^3 + \varepsilon^4 \leq (1 + \varepsilon)^4$. Part 4 is similar to Part 2.

Thus, we have found that

$$\varepsilon \leq 6b_1 \left|\left|1 - r^4\right|\right|_{\mathcal{E}}^{1/2} (\eta + 2d) \leq 6b_1(\eta + 2d)(1 + \varepsilon)^2.$$

A straightforward calculation with this result then shows that $\varepsilon \leq 24b_1(\eta + 2d)$, which implies the first statement of the lemma. To prove the second statement, we use the fact that $\|1 - r^4\|_{\mathcal{D}_0}^{1/2} \leq (1 + \varepsilon)^2 \leq [1 + 24b_1(\eta + 2d)]^2$, as already shown. □

Lemma 19. *Assume that (13), (14), (15), and (17) hold. Then,*

$$\|g\|_{\mathcal{D}_0} \leq \frac{2^{-4/3}}{27} b_1^{-4/3} (1-L)^{-5/3} L^2 M^{1/3}, \tag{30}$$

$$\|F\|_{\mathcal{D}_0} \leq \nu d b_1^{-4/3} b_2 \frac{M^{1/3}}{\log(M)}. \tag{31}$$

Proof. The assumption on M implies that $\log M > 0$. As in the proof of Lemma 17, $\|b_2 J/\log(M)\|_{\mathcal{D}_0} \leq L < 1$, and the result then follows from Lemma 16 and Lemma 18. Condition (15) implies that $\|F_1\|_{\mathcal{D}_0} \leq \|F_2\|_{\mathcal{D}_0}$, and (17) bounds $\|z_2\|_{\mathcal{D}_0}$. □

Lemma 20. *Assume that $\nu \leq \frac{1}{9} \cdot 2^{-7/3}$ and $\gamma = \eta/18 \leq \frac{49}{72}$, as in Theorem 6. If conditions (13)–(17) hold, then*

$$\omega_0 \leq \frac{A}{\log(2)} \left(\frac{1}{3} + \frac{\log(B)}{\log(M)} \right) M^{1/3}.$$

Theorem 6 now follows immediately from this lemma and the expression for $\omega = K'(I_0)$.

Proof. By the previous lemma,

$$C \leq \frac{2}{3} \max \left\{ \frac{\eta}{3} + \left(\frac{2^{-1/3}}{9} + \nu \right) d b_1^{-4/3} b_2 \frac{M^{1/3}}{\log(M)} + \frac{2^{-4/3}}{27} b_1^{-4/3} (1-L)^{-5/3} L^2 M^{1/3}, 1 \right\}.$$

A straightforward calculation shows that $\nu \leq \frac{1}{9} \cdot 2^{-7/3}$ implies $2\|F\|_{\mathcal{D}_0} \leq md$. Hence,

$$\begin{aligned}
\alpha_0 &= \frac{3 + 12(\eta + 2d)}{2d} (\|F\|_{\mathcal{D}_0} + 2C) \\
&\leq \frac{1 + 4(\eta + 2d)}{d} \max \left\{ \frac{2\eta}{3} M^{-1/3} \log(M) + \left(\frac{2^{2/3}}{9} + \frac{7\nu}{2} \right) d b_1^{-4/3} b_2 \right. \\
&\qquad + \frac{2^{-1/3}}{27} b_1^{-4/3} (1-L)^{-5/3} L^2 \log(M), 2M^{-1/3} \log(M) \\
&\qquad \left. + \frac{3\nu}{2} d b_1^{-4/3} b_2 \right\} \frac{M^{1/3}}{\log(M)} \\
&= A \frac{M^{1/3}}{\log(M)}.
\end{aligned}$$

From $\gamma = \eta/18 \leq 49/72$, it follows that $12 \leq \frac{1}{108} \cdot 7^8 (\eta - 6\gamma)^{-4}$. We observe that γ does not appear in any other quantity besides b. The choice $\gamma = \eta/18$ minimizes b. We obtain

$$\begin{aligned}
b &= \frac{7^8 \cdot 18^2 \cdot 3^4 (2 + 3m)}{108 \cdot 2^4 c \eta^6} md \\
&= 2^{-4} \cdot 3^5 \cdot 7^8 c^{-1} \eta^{-6} (2 + 3m) md
\end{aligned}$$

$$= 2^{-13/3} \cdot 3^3 \cdot 7^8 c^{-1} d b_1^{-4/3} b_2 \eta^{-6} \left(\frac{1}{\log(M)} + \frac{2^{-7/3}}{3} b_1^{-4/3} b_2 \frac{M^{1/3}}{\log^2(M)} \right) M^{1/3}$$

$$= BM^{1/3}.$$

From $b \geq 2$, we see that $L_W(b \log(2)) \leq \log(b)$. The result follows. □

Remark 21. The transformation $I \mapsto J$ is chosen so that ω and ω_0 have the same growth rate in I_0 and z_4 (i.e., in the leading term). Independent of the rescaling, ω grows as $I_0^{1/3}$. On the other hand, $\omega_0 \leq \alpha_0 \log(b)/\log(2)$ (if $b \geq 2$). Because b grows as some power of I_0, it follows that α_0 must grow as $I_0^{1/3}/\log(I_0)$. Analyzing the dependence on z_4 then leads to the chosen rescaling.

5. Summary and Conclusions

In this paper, we discussed quasiperiodic dynamics in Bose-Einstein condensates (BECs) in periodic lattices and superlattices. The mean-field dynamics of a BEC is governed by the Gross-Pitaevskii (GP) equation (1), which consists of a cubic nonlinear Schrödinger equation plus an external potential that takes into account the "trap" where the condensate resides. In this mean-field description, a given particle in the BEC is affected by the other particles only through average effects, and the nonlocal term in the original many-body Hamiltonian leads to the nonlinear term in the GP equation. One obtains a cubic nonlinearity if considering only two-body interactions. The GP equation, which is derived as a zero-temperature theory, provides a good description for BEC dynamics below the critical transition temperature at which the condensate forms [17], [33]. In "cigar-shaped" BECs, two dimensions are tightly confined, so one may further reduce (1) to (2), which has one spatial dimension [17]. The amplitude dynamics of coherent structures of (2) with trivial phase (which describe standing waves) are governed by a forced Duffing equation given by (8), or equivalently by (9). The first equation arises directly from the physical setting, whereas (9) is the more convenient decription for mathematical analysis. We briefly describe the dynamics of this system.

In the absence of the forcing (i.e., when the external potential $V \equiv 0$), the system reduces to the autonomous Duffing oscillator and is integrable. Its dynamics depends on the sign of the chemical potential μ (which indicates how many particles are trapped in the BEC) and is illustrated in Figure 4. Here, we considered the two situations with negative chemical potential (Figure 4b,c). In both cases, there is a family of invariant tori winding around the trivial periodic orbit $R \equiv 0$. When viewed in the proper coordinates, the dynamics on each torus is a flow with constant velocity vector. One frequency is equal to 1, and the other varies from one torus to the next, going to infinity monotonically as the distance of the torus to $R \equiv 0$ goes to infinity. The "proper coordinates" are the action-angle coordinates introduced in Section 4. These tori correspond to quasiperiodic oscillations of $R(x)$, which describes the amplitude dynamics of the BEC wave function. We note that in this unforced setting, the quasiperiodicity has no physical meaning, as the period of the optical lattice potential does not yet play a role.

In the forced setting, $V \neq 0$. Figures 1 to 3 illustrate the case of a periodic lattice for a range of amplitudes. We remark that from a mathematical point of view, there is no extra difficulty in dealing with superlattices or even lattices with more than two Fourier modes as compared to lattices with just a single mode, provided the periods are commensurate (that is, provided they have a common multiple). Our main result, Theorem 6, uses KAM theory to demonstrate that for any size of the periodic forcing, there exist invariant tori winding around the trivial periodic orbit. Let $R_{\max}$ denote the maximal R coordinate on an invariant torus. That is, $R_{\max}$ is the amplitude of the corresponding oscillations. In terms of the mathematical setting (9), invariant tori exist for a dense set of "admissible" $R_{\max}$ in the interval $(cz_4^{-1/2}\|z_2\|^{1/2}, +\infty)$ for some positive constant $c > 0$. In terms of the physical parameters, the lowest admissible amplitude is roughly equal to $3b_1\hbar\kappa\omega/(\pi\sqrt{-mg})$, where ω is its frequency, κ is the lattice wave number, $b_1 \approx 0.874019$ is a constant, m is the mass of the atomic species in the condensate, and $g < 0$ is the scaled value of the two-body scattering length. The parameter g varies from one condensate species to another and can be changed by exploiting Feshbach resonances [21].

The set of admissible $R_{\max}$ is characterized by a Diophantine condition on the frequencies of the torus. A slightly different KAM theorem than the one used in this work shows that, for each forcing, the relative measure of invariant tori converges to full measure as $R_{\max} \to +\infty$. See, for example, [47], [58] for a general statement or [8] for discussion of a system similar to ours. Thus, we find a large measure of quasiperiodic dynamics, and in the complement of the union of invariant tori, there exist Aubry-Mather sets. Furthermore, by the Poincaré-Birkhoff theorem [5], [6], in between any two invariant tori there are periodic orbits of saddle and center type for all intermediate resonant frequencies (technically, these can be classified as Aubry-Mather sets as well). As a result, there is a large measure of quasiperiodic invariant tori interlaced with Aubry-Mather sets and resonant layers. We further note that the homoclinic figure eight that exists in the unforced setting for $\mu < 0$ will generically break under the forcing, generating a homoclinic tangle, as can be checked for this specific case by computing Melnikov integrals. We refer to [25], [64] for such computations on similar systems. A possible direction for future study would be to establish conditions for the nonexistence of invariant tori in the system under consideration, which would complement the existence conditions presented in this paper. Such a *converse KAM theorem* was obtained in [41] for area-preserving twist maps and in [39] in a Lagrangian/Hamiltonian setting.

From a physical perspective, we recall that the GP equation is derived from a many-body quantum problem under the assumption that the Bose gas is dilute [17], [33]. In particular, this implies that the mean interparticle distance should be much larger than the scattering length. Therefore, the large R results obtained here would necessitate the condensate to have expanded sufficiently to ensure that its density is low (so that the reduction from the many-body problem to the three-dimensional GP description remains valid). Accordingly, for sufficiently large R, one would eventually have to include corrections to the GP equation arising beyond the mean-field description to describe the physics correctly. Incorporating beyond-mean-field dynamics in the study of BECs is a difficult problem (see, e.g., the discussion in [59]), and it is not agreed precisely when such corrections become relevant or what form they should take to simultaneously ensure tractability and correctly capture the physics.

Acknowledgments

We are grateful to Peter Engels, Panos Kevrekidis, Boris Malomed, Alexandru Nicolin, and Li You for useful discussions concerning this research. We also thank the editor and an anonymous referee whose constructive comments led to significant improvement of this manuscript. MAP was supported in part by a VIGRE grant awarded to the School of Mathematics at Georgia Tech and in part by the Gordon and Betty Moore Foundation through Caltech's Center for the Physics of Information. MvN was partially supported by the Center for Dynamical Systems and Nonlinear Studies at Georgia Tech and partially by EPSRC grant GR/S97965/01. YY was partially supported by NSF grant DMS0204119.

References

[1] B. P. Anderson and M. A. Kasevich. Macroscopic quantum interference from atomic tunnel arrays. *Science*, 282(5394):1686–1689, 1998.

[2] M. H. Anderson, J. R. Ensher, M. R. Matthews, C. E. Wieman, and E. A. Cornell. Observation of Bose-Einstein condensation in a dilute atomic vapor. *Science*, 269(5221):198–201, 1995.

[3] V. I. Arnol'd. Small denominators and problems of stability of motion in classical and celestial mechanics. *Uspehi Mat. Nauk*, 18(6 (114)):91–192, 1963. Translated in *Russian Math. Surveys*.

[4] S. Aubry and P. Y. Le Daeron. The discrete Frenkel-Kontorova model and its extensions. I. Exact results for the ground-states. *Physica D*, 8(3):381–422, 1983.

[5] G. D. Birkhoff. Proof of Poincaré's geometric theorem. *Trans. Amer. Math. Soc.*, 14(1):14–22, 1913.

[6] G. D. Birkhoff. An extension of Poincaré's last geometric theorem. *Acta Mathematica*, 47:297–311, 1925.

[7] H. W. Broer, I. Hoveijn, M. van Noort, C. Simó, and G. Vegter. The parametrically forced pendulum: A case study in $1\frac{1}{2}$ degree of freedom. *J. Dynam. Diff. Eq.*, 16(4):897–947, 2004.

[8] H. W. Broer, M. van Noort, and C. Simó. Existence and measure of 2-quasiperiodicity in Hamiltonian one-and-a-half degree of freedom systems. In *Equadiff—International Conference on Differential Equations, Hasselt 2003*, pages 595–600. World Scientific, 2005.

[9] J. C. Bronski, L. D. Carr, R. Carretero-González, B. Deconinck, J. N. Kutz, and K. Promislow. Stability of attractive Bose-Einstein condensates in a periodic potential. *Phys. Rev. E*, 64(056615), 2001.

[10] J. C. Bronski, L. D. Carr, B. Deconinck, and J. N. Kutz. Bose-Einstein condensates in standing waves: The cubic nonlinear Schrödinger equation with a periodic potential. *Phys. Rev. Lett.*, 86(8):1402–1405, February 2001.

[11] J. C. Bronski, L. D. Carr, B. Deconinck, J. N. Kutz, and K. Promislow. Stability of repulsive Bose-Einstein condensates in a periodic potential. *Phys. Rev. E*, 63(036612), 2001.

[12] R. Carretero-González and K. Promislow. Localized breathing oscillations of Bose-Einstein condensates in periodic traps. *Phys. Rev. A*, 66(033610), 2002.

[13] F. S. Cataliotti, L. Fallani, F. Ferlaino, C. Fort, P. Maddaloni, and M. Inguscio. Superfluid current disruption in a chain of weakly coupled Bose-Einstein condensates. *New J. Phys.*, 5(71), 2003.

[14] G. Chong, W. Hai, and Q. Xie. Spatial chaos of trapped Bose-Einstein condensate in one-dimensional weak optical lattice potential. *Chaos*, 14(2):217–223, 2004.

[15] S.-N. Chow, M. van Noort, and Y. Yi. Quasiperiodic dynamics in Hamiltonian $1\frac{1}{2}$ degree of freedom systems far from integrability. *J. Diff. Eq.*, 212(2):366–393, 2005.

[16] V. P. Chua and M. A. Porter. Spatial resonance overlap in Bose-Einstein condensates in optical superlattices. *Int. J. Bifurc. Chaos*, 16:945–959.
[17] F. Dalfovo, S. Giorgini, L. P. Pitaevskii, and S. Stringari. Theory of Bose-Einstein condensation in trapped gases. *Rev. Mod. Phys.*, 71(3):463–512, 1999.
[18] K. B. Davis, M.-O. Mewes, M. R. Andrews, N. J. van Druten, D. S. Durfee, D. M. Kurn, and W. Ketterle. Bose-Einstein condensation in a gas of sodium atoms. *Phys. Rev. Lett.*, 75(22):3969–3973, 1995.
[19] J. Hecker Denschlag, J. E. Simsarian, H. Häffner, C. McKenzie, A. Browaeys, D. Cho, K. Helmerson, S. L. Rolston, and W. D. Phillips. A Bose-Einstein condensate in an optical lattice. *J. Phys. B: Atomic Molecular and Optical Physics*, 35:3095–3110, 2002.
[20] R. Dieckerhoff and E. Zehnder. Boundedness of solutions via the twist-theorem. *Ann. Scuola Norm. Sup. Pisa Cl. Sci. (4)*, 14(1):79–95, 1987.
[21] E. A. Donley, N. R. Claussen, S. L. Cornish, J. L. Roberts, E. A. Cornell, and C. E. Weiman. Dynamics of collapsing and exploding Bose-Einstein condensates. *Nature*, 412:295–299, 2001.
[22] Y. Eksioglu, P. Vignolo, and M. P. Tosi. Matter-wave interferometry in periodic and quasiperiodic arrays. *Optics Commun.*, 243(1–6):175–181, 2004.
[23] N. Gemelke, E. Sarajlic, Y. Bidel, S. Hong, and S. Chu. Parametric amplification of matter waves in periodically translated optical lattices. *Phys. Rev. Lett.*, 95(170404), 2005.
[24] M. Greiner, O. Mandel, T. Esslinger, T. Hänsch, and I. Bloch. Quantum phase transition from a superfluid to a Mott insulator in a gas of ultracold atoms. *Nature*, 415(6867):39–44, 2002.
[25] J. Guckenheimer and P. Holmes. *Nonlinear Oscillations, Dynamical Systems, and Bifurcations of Vector Fields*. Number 42 in Applied Mathematical Sciences. Springer-Verlag, New York, 1983.
[26] E. W. Hagley, L. Deng, M. Kozuma, J. Wen, K. Helmerson, S. L. Rolston, and W. D. Phillips. A well-collimated quasi-continuous atom laser. *Science*, 283(5408):1706–1709, 1999.
[27] M. R. Herman. *Sur les courbes invariantes par les difféomorphismes de l'anneau, vol. 1*, volume 103–104 of *Astérisque*. Société Mathématique de France, 1983.
[28] M. R. Herman. *Sur les courbes invariantes par les difféomorphismes de l'anneau, vol. 2*, volume 144 of *Astérisque*. Société Mathématique de France, 1986.
[29] H. Huang. Destruction of invariant tori in pendulum-type equations. *J. Diff. Eq.*, 146(1):67–89, 1998.
[30] P. G. Kevrekidis, G. Theocharis, D. J. Frantzeskakis, and B. A. Malomed. Feshbach resonance management for Bose-Einstein condensates. *Phys. Rev. Lett.*, 90:230401, 2003.
[31] M. Levi. Quasiperiodic motions in superquadratic time-periodic potentials. *Commun. Math. Phys.*, 143(1):43–83, 1991.
[32] M. Levi and E. Zehnder. Boundedness of solutions for quasiperiodic potentials. *SIAM J. Math. Anal.*, 26(5):1233–1256, 1995.
[33] E. H. Lieb, R. Seiringer, J. P. Solovej, and J. Yngvason. *The Mathematics of the Bose Gas and Its Condensation*. Birkäuser, Basel, Germany, 2005.
[34] J. E. Littlewood. Unbounded solutions of an equation $\ddot{y} + g(y) = p(t)$, with $p(t)$ periodic and bounded, and $g(y)/y \to \infty$ as $y \to \pm\infty$. *J. London Math. Soc.*, 41:491–507, 1966.
[35] B. Liu. Boundedness for solutions of nonlinear Hill's equations with periodic forcing terms via Moser's twist theorem. *J. Diff. Eq.*, 79(2):304–315, 1989.
[36] P. J. Y. Louis, E. A. Ostrovskaya, and Y. S. Kivshar. Matter-wave dark solitons in optical lattices. *J. Optics B: Quantum and Semiclassical Optics*, 6:S309–S317, 2004.
[37] P. J. Y. Louis, E. A. Ostrovskaya, C. M. Savage, and Y. S. Kivshar. Bose-Einstein condensates in optical lattices: Band-gap structure and solitons. *Phys. Rev. A*, 67(013602), 2003.
[38] M. Machholm, A. Nicolin, C. J. Pethick, and H. Smith. Spatial period-doubling in Bose-Einstein condensates in an optical lattice. *Phys. Rev. A*, 69(043604), 2004.
[39] R. S. MacKay. A criterion for nonexistence of invariant tori for Hamiltonian systems. *Physica D*, 36(1-2):64–82, 1989.
[40] J. N. Mather. Existence of quasiperiodic orbits for twist homeomorphisms of the annulus. *Topology*, 21(4):457–467, 1982.

[41] J. N. Mather. Nonexistence of invariant circles. *Ergodic Theory Dynam. Syst.*, 4(2):301–309, 1984.
[42] C. Menotti, A. Smerzi, and A. Trombettoni. Superfluid dynamics of a Bose-Einstein condensate in a periodic potential. *New J. Phys.*, 5(112), 2003.
[43] O. Morsch, J. H. Müller, M. Christiani, D. Ciampini, and E. Arimondo. Bloch oscillations and mean-field effects of Bose-Einstein condensates in 1D optical lattices. *Phys. Rev. Lett.*, 87(140402), September 2001.
[44] J. Moser. Recent developments in the theory of Hamiltonian systems. *SIAM Rev.*, 28(4):459–485, 1986.
[45] J. Moser. Minimal foliations on a torus. In M. Giaquinta, editor, *Topics in calculus of variations (Montecatini Terme, 1987)*, volume 1365 of *Lecture Notes in Mathematics*, pages 62–99. Springer-Verlag, New York, 1989.
[46] J. Moser. Quasi-periodic solutions of nonlinear elliptic partial differential equations. *Bol. Soc. Brasil. Mat. (N.S.)*, 20(1):29–45, 1989.
[47] A. I. Neishtadt. Estimates in the Kolmogorov theorem on conservation of conditionally periodic motions. *J. Appl. Math. Mech.*, 45(6):1016–1025, 1981.
[48] A. I. Neishtadt, V. V. Sidorenko, and D. V. Treschev. Stable periodic motions in the problem on passage through a separatrix. *Chaos*, 7(1):2–11, 1997.
[49] C. Orzel, A. K. Tuchman, M. L. Fenselau, M. Yasuda, and M. A. Kasevich. Squeezed states in a Bose-Einstein condensate. *Science*, 291(5512):2386, 2001.
[50] P. Pedri, L. Pitaevskii, S. Stringari, C. Fort, S. Burger, F. S. Cataliotii, P. Maddaloni, F. Minardi, and M. Inguscio. Expansion of a coherent array of Bose-Einstein condensates. *Phys. Rev. Lett.*, 87(22):220401, 2001.
[51] S. Peil, J. V. Porto, B. Laburthe Tolra, J. M. Obrecht, B. E. King, M. Subbotin, S. L. Rolston, and W. D. Phillips. Patterned loading of a Bose-Einstein condensate into an optical lattice. *Phys. Rev. A*, 67(051603(R)), 2003.
[52] M. A. Porter and P. Cvitanović. Modulated amplitude waves in Bose-Einstein condensates. *Phys. Rev. E*, 69(047201), 2004.
[53] M. A. Porter and P. Cvitanović. A perturbative analysis of modulated amplitude waves in Bose-Einstein condensates. *Chaos*, 14(3):739–755, 2004.
[54] M. A. Porter and P. G. Kevrekidis. Bose-Einstein condensates in superlattices. *SIAM J. Appl. Dynam. Syst.*, 4(4):783–807, 2005.
[55] M. A. Porter, P. G. Kevrekidis, R. Carretero-González, and D. J. Frantzeskakis. Dynamics and manipulation of matter-wave solitons in optical superlattices. *Phys. Lett. A*, 352:210–215, 2006.
[56] M. A. Porter, P. G. Kevrekidis, and B. A. Malomed. Resonant and non-resonant modulated amplitude waves for binary Bose-Einstein condensates in optical lattices. *Physica D*, 196(1–2):106–123, 2004.
[57] J. V. Porto, S. Rolston, B. Laburthe Tolra, C. J. Williams, and W. D. Phillips. Quantum information with neutral atoms as qubits. *Phil. Trans.: Math., Physical & Engin. Sci.*, 361(1808):1417–1427, 2003.
[58] J. Pöschel. The concept of integrability on Cantor sets for Hamiltonian systems. *Celestial Mech.*, 28(1–2):133–139, 1982.
[59] A. M. Rey, B. L. Hu, E. Calzetta, A. Roura, and C. Clark. Nonequilibrium dynamics of optical lattice-loaded BEC atoms: Beyond HFB approximation. *Phys. Rev. A*, 69:033610, 2004.
[60] L. Salasnich, A. Parola, and L. Reatto. Periodic quantum tunnelling and parametric resonance with cigar-shaped Bose-Einstein condensates. *J. Phys. B: Atomic Molecular and Optical Physics*, 35(14):3205–3216, 2002.
[61] A. Smerzi, A. Trombettoni, P. G. Kevrekidis, and A. R. Bishop. Dynamical superfluid-insulator transition in a chain of weakly coupled Bose-Einstein condensates. *Phys. Rev. Lett.*, 89:170402, 2002.
[62] Q. Thommen, J. C. Garreau, and V. Zehnlé. Classical chaos with Bose-Einstein condensates in tilted optical lattices. *Phys. Rev. Lett.*, 91:210405, 2003.

[63] K. G. H. Vollbrecht, E. Solano, and J. L. Cirac. Ensemble quantum computation with atoms in periodic potentials. *Phys. Rev. Lett.*, 93(220502), 2004.
[64] S. Wiggins. *Global Bifurcations and Chaos. Analytical Methods*, Volume 73 of *Applied Mathematical Sciences*. Springer-Verlag, New York, 1988.
[65] B. Wu, R. B. Diener, and Q. Niu. Bloch waves and Bloch bands of Bose-Einstein condensates in optical lattices. *Phys. Rev. A*, 65(025601), 2002.
[66] J. You. Invariant tori and Lagrange stability of pendulum-type equations. *J. Diff. Eq.*, 85:54–65, 1990.